

Electronic Supplementary Information
for

**An isoelectronic NO dioxygenase reaction using a nonheme
iron(III)-peroxo complex and nitrosonium ion**

Atsutoshi Yokoyama,^a Jung Eun Han,^a Kenneth D. Karlin,^{*,a,b} and Wonwoo Nam^{*,a}

^aDepartment of Chemistry and Nano Science, Department of Bioinspired Science, Ewha
Womans University, Seoul 120-750, Korea

^bDepartment of Chemistry, The Johns Hopkins University, Baltimore, MD 21218, USA

E-mails: karlin@jhu.edu, wwnam@ewha.ac.kr

Table of Contents

Experimental Section

Materials and Instrumentation	S3
Purification of Nitrogen Dioxide	S4
Synthesis of [Fe(14-TMC)(O ₂)]OTf (1 •OTf)	S5
Synthesis of [Fe(14-TMC)(O)(CH ₃ CN)](OTf) ₂ (5 •(OTf) ₂).	S5
Synthesis of [Fe(14-TMC)(O)(F)](OTf) (7 •OTf)	S5
Reaction of Fe(III)-Peroxo Complex (1) and Nitrosonium ion (NO ⁺)	S6
Reaction of Fe(IV)-Oxo Complex (4) and NO ₂	S6
Reaction of Fe(IV)-Oxo Complex Bonding Fluoride Axial Ligand (7) and NO ₂	S6
Nitration of 2,4-Di- <i>t</i> -butylphenol (DTBP)	S7
References	S7
Figure S1 EPR spectrum of [Fe(14-TMC)(NO ₃)(F)] ⁺ .	S9
Figure S2 UV-vis spectral changes of [Fe(14-TMC)(O ₂)] ⁺ with 1.2 equiv. of NOPF ₆ followed by the addition of DTBP.	S10
Figure S3 EPR spectrum of [Fe(14-TMC)(OH)(F)] ⁺ .	S11
Figure S4 UV-vis spectral changes of [Fe(14-TMC)(O)(CH ₃ CN)] ²⁺ upon addition of NO ₂ .	S12
Figure S5 EPR spectra of [Fe(14-TMC)(NO ₃)] ⁺ and [Fe(14-TMC)(NO ₃)(F)] ⁺ .	S13
Figure S6 EPR spectrum of [Fe(14-TMC)(NO ₃)(F)] ⁺ .	S14
Figure S7 UV-vis spectrum and ESI-MS of [Fe(14-TMC)(O)(F)] ⁺ .	S15
Figure S8 UV-vis spectral changes of [Fe(14-TMC)(O)(F)] ⁺ upon addition of NO ₂ .	S16
Figure S9 EPR spectrum of [Fe(14-TMC)(NO ₃)(F)] ⁺ .	S17
Figure S10 Cyclic voltammogram of [Fe(14-TMC)(O)(F)](OTf).	S18

Experimental Section

Materials and Instrumentation. All chemicals obtained from Aldrich Chemical Co. were of the best available purity and used without further purification unless otherwise indicated. Solvents were dried according to published procedures and distilled under Ar prior to use.^{S1} The $[\text{Fe}(14\text{-TMC})(\text{OTf})_2]$ (14-TMC = 1,4,8,11-tetramethyl-1,4,8,11-tetraazacyclotetradecane) complex was prepared in a dry box according to the literature methods.^{S2} Iodosylbenzene (PhIO) was prepared from iodobenzene diacetate according to a literature procedure.^{S3} Air-sensitive reactions with iron complexes were performed using either a dry box or standard Schlenk techniques. UV-vis spectra were recorded on a Hewlett-Packard 8453 diode array spectrophotometer equipped with a UNISOKU Scientific Instruments for low-temperature experiments. Electrospray ionization mass spectra (ESI-MS) were collected on a Thermo Finnigan (San Jose, CA, USA) LCQTM Advantage MAX quadrupole ion trap instrument, by infusing samples directly into the source using a manual method. The spray voltage was set at 4.2 kV and the capillary temperature at 80 °C. EPR spectra were taken at 5 K using an X-band Bruker EMX-plus spectrometer equipped with a dual mode cavity (ER 4116DM). Low temperatures were achieved and controlled using an Oxford Instruments ESR900 liquid He quartz cryostat with an Oxford Instruments ITC503 temperature and gas flow controller. Product analysis was performed with an Agilent Technologies 6890N gas chromatograph (GC). Cyclic voltammetry (CV) measurements were performed on an ALS 630B electrochemical analyzer, and voltammograms were measured in deaerated CH_3CN containing 0.1 M TBAPF_6 as a supporting electrolyte at -10 °C, with use of Pt electrode as working electrode, Ag/AgNO_3 as a reference electrode and a Pt wire as a counter electrode. The Pt working electrode was routinely polished with BAS polishing

alumina suspension and rinsed with CH₃CN before use. The potentials were measured with respect to the Ag/AgNO₃ (10 mM) reference electrode and were converted to values vs SCE by adding 0.29 V.^{S4} All electrochemical measurements were carried out under an atmospheric pressure of Ar. The yield of nitrate was determined by using QUANTOFIX[®] Nitrate/Nitrite testing tips (MACHEREY-NAGEL, Germany) and sodium nitrate solution was used as authentic samples; 1.0, 2.0, 3.0, 4.0, 5.0 and 6.0 mM aqueous solutions of NaNO₃ were prepared and the color change of the testing tips were recorded in each solution as a prior analysis. After the reaction, the solvent was removed and dried under vacuo. The resulting compound was redissolved in dichloromethane and extracted with known amount of sodium chloride solution (i.e., 0.5 mL) and checked the color of the testing tips (Note to use 6 mM as a maximum concentration.). The color comparison of the tips of resulting solution with that of NaNO₃ solutions gives the concentration of nitrate ion obtained, which then is converted to the yield of nitrate ion.

Purification of Nitrogen Dioxide. Nitrogen dioxide gas (NO₂) was obtained from Dong-A Specialty Gases and purified as follows: NO₂ was trapped into a Schlenk flask using liquid N₂ and the frozen NO₂ (as crystalline N₂O₄) was warmed with an acetone/dry-ice bath (−80 °C) to eliminate the impurity (e.g., nitric oxide). CH₃CN (15 mM) was added to the purified NO₂ and kept for 30 min in a closed Schlenk flask at room temperature. The concentration of the NO₂-CH₃CN was determined by the spectroscopic absorptivity value for NO₂ in CH₃CN ($\epsilon = 64 \text{ M}^{-1} \text{ cm}^{-1}$ at 372 nm at −40 °C). The ϵ value of NO₂ in CH₃CN was determined from the reaction of purified nitric oxide (NO)^{S5} and dioxygen gas (O₂(g)) in

CH₃CN at -40 °C. Then, the appropriate amount of NO₂-CH₃CN was added to reactant by gas-tight syringe.

Synthesis of [Fe(14-TMC)(O₂)]OTf (1).^{S6} Treatment of [Fe(14-TMC)(OTf)₂] (69.3 mg, 0.1 mmol) with 2 equiv. of tetraethylammonium hydroxide (28 μL, 0.2 mmol) and 5 equiv. of H₂O₂ (51 μL, 0.5 mmol) in 2 mL of CH₃CN at -20 °C afforded the formation of a bluish-green solution. Cold Et₂O (40 mL) was added to the solution at -40 °C to precipitate purple product. The solvent was removed and the purple product was washed with cold Et₂O several times. Then, the purple product was dried in vacuo. Yield: 80% (3.95 mg, 0.08 mmol). UV-vis (ε, M⁻¹ cm⁻¹) in CH₃CN at -10 °C: 868 nm (600).

Synthesis of [Fe(14-TMC)(O)(CH₃CN)](OTf)₂ (5).^{S6} [Fe^{II}(14-TMC)(OTf)₂] (50mg, 78 μmol) was dissolved in CH₃CN (1 mL) at room temperature, and iodosylbenzene (20 mg, 227 μmol) was added. The solution was stirred for 1 h at room temperature and filtered. To this filtrate, cold Et₂O (50 mL) was added at -40 °C to precipitate green product, and the solvent was removed. After washing with cold Et₂O (50 mL) several times, the green product was dried under vacuum at -40 °C. Yield: 58% (30 mg, 45 μmol). UV-vis (ε, M⁻¹ cm⁻¹) in CH₃CN at -10 °C: 820 nm (400).

Synthesis of [Fe(14-TMC)(O)(F)](OTf) (7). The Complex **5** (30mg, 45 μmol) was dissolved in 0.5 mL of CH₃CN at -30 °C, and tetrabutylammonium fluoride (TBAF) (15 mg, 54 μmol) in 0.5 mL of CH₃CN was added. After addition of TBAF, the color of the solution changed from green to orange. Addition of cold Et₂O (20 mL) to the reaction mixture resulted in an orange precipitate, and the solvent was then removed. The resulted orange solid was

washed with Et₂O several times, and dried under vacuum. Yield: 90% (20 mg, 40 μmol). UV-vis (ϵ , M⁻¹ cm⁻¹) in CH₃CN at -10 °C: 812 nm (53), 1015 (69) (Figure S7).

Reactivity Study. All reactions were run in an UV cuvette and monitored using UV-vis spectroscopy on the reaction solutions. Reactions were run at least in triplicate, and the data reported represents the average results observed for these reactions. Preparation of samples and all reaction experiments with nitrosonium hexafluorophosphate (NOPF₆) were performed under an inert gas in a dry box. The purity of 2,4-di-*tert*-butylphenol (DTBP) was checked with GC prior to use. Products were analyzed by injecting the reaction mixture directly into GC. Products were identified by comparing with authentic samples, and product yields were determined by comparison against standard curves prepared with authentic samples and using decane as an internal standard.

Reaction of Fe(III)-Peroxo Complex (1) and Nitrosonium Ion (NO⁺). [Fe(14-TMC)(O₂)](OTf) (1) was dissolved in CH₃CN (1 mM) at -10 °C under Ar, and 1.2 equiv. of NOPF₆ (1 mM) was added under Ar. UV-vis spectroscopy was used to monitor the reaction (Figure 1a). The yield of nitrate was estimated to be 67%.

Reaction of Fe(IV)-Oxo Complex (4) and NO₂. To the complex 4 (1 mM, 2 mL) in CH₃CN at -10 °C under Ar in the presence and absence of 1 mM TBAPF₆, 5 equiv. of NO₂ was added and stirred for 30 min. UV-vis spectral changes were monitored and depicted in Figure S4. To this solution, 1.2 equiv. of TBAF (tetrabutylammonium fluoride) was added and stirred for 30 min. The yield of nitrate was estimated as 67%.

Reaction of Fe(IV)-Oxo Complex Bonding Fluoride Axial Ligand (7) and NO₂. NO₂ (5 equiv.) was added to the solution of 7 (1 mM, 2 mL) in CH₃CN at -10 °C under Ar, and its

UV-vis spectral changes were monitored (Figure S8). The yield of nitrate was estimated to be 67%.

Nitration of 2,4-Di-*t*-Butylphenol (DTBP). The reaction was carried out in a closed system. The solution of NOPF_6 (1.2 mM) was prepared in an UV cuvette fitted with a septum at $-10\text{ }^\circ\text{C}$ under Ar. To this solution, $[\text{Fe}(14\text{-TMC})(\text{O}_2)]^+$ (**1**) (1 mM) in CH_3CN was added by a gas tight syringe. Subsequent to the formation of the Fe(IV)-oxo complex, $[\text{Fe}(14\text{-TMC})(\text{O})]^{2+}$ (**2**), 2 equiv. of DTBP in CH_3CN were added by a gas tight syringe and stirred for 20 min. Product analysis was performed by GC, and it was found that 2,4-di-*t*-butyl-6-nitrophenol (nitro-DTBP) and 3,3',5,5'-tetra-*t*-butyl-(1,1'-biphenyl)-2,2'-diol (DTBP-dimer) formed in 65% and 3% yield, respectively (Figure S2). When the above reaction was carried out in an open UV cuvette, nitro-DTBP and DTBP-dimer were found to be formed in 38% and 0% yield, respectively.

References

- S1. *Purification of Laboratory Chemicals*; Armarego, W. L. F., Perrin, D. D., Eds; Pergamon Press: Oxford, 1997.
- S2. J.-U. Rohde, J.-H. In, M. H. Lim, W. W. Brennessel, M. R. Bukowski, A. Stubna, E. Müunck, W. Nam, L. Que Jr., *Science* 2003, **299**, 1037.
- S3. H. Sahzman, J. G. Sharefkin, *Organic Synthesis*, Collect. 5th ed., Wiley: New York, 1973.
- S4. Mann, C. K.; Barnes, K. K. *Electrochemical Reactions in Nonaqueous Systems*; Marcel Dekker: New York, 1990.

S5. For purification of nitric oxide, see: A. Yokoyama, K.-B. Cho, K. D. Karlin, W. Nam, *J.*

Am. Chem. Soc., 2013, **135**, 14900.

S6. (a) J. Cho, S. Jeon, S. A. Wilson, L. V. Liu, E. A. Kang, J. J. Braymer, M. H. Lim, B.

Hedman, K. O. Hodgson, J. S. Valentine, E. I. Solomon, W. Nam, *Nature* 2011, **478**, 502.

(b) J. Annaraj, Y. Suh, M. S. Seo, S. O. Kim, W. Nam, *Chem. Commun.* 2005, 4529. (c)

M. S. Seo, J. Y. Kim, J. Annaraj, Y. Kim, Y.-M. Lee, S.-J. Kim, J. Kim, W. Nam, *Angew.*

Chem. Int. Ed. 2007, **46**, 377. (d) W. L. F. Armarego, C. L. L. Chai, *Purification of*

Laboratory Chemicals, 5th ed., Butterworth-Heiemann, Oxford, 2003.

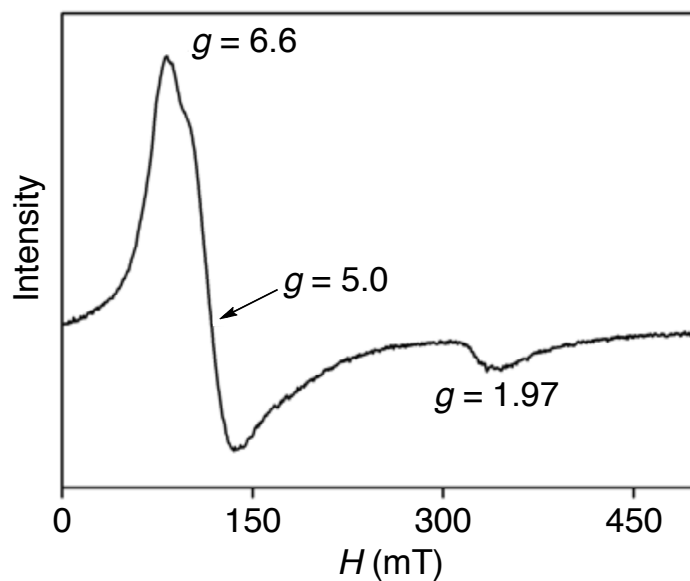


Fig. S1. EPR spectrum of the reaction solution of $[\text{Fe}(14\text{-TMC})(\text{O}_2)]^+$ (**1**) (1 mM) and 1.2 equiv. of NOPF_6 in CH_3CN at 5 K. Experimental parameters: Power, 1.0 mW; Frequency, 9.647 GHz; Receive Gain, 1.0×10^4 ; Modulation Frequency, 100 kHz; Modulation Amplitude, 10 G.

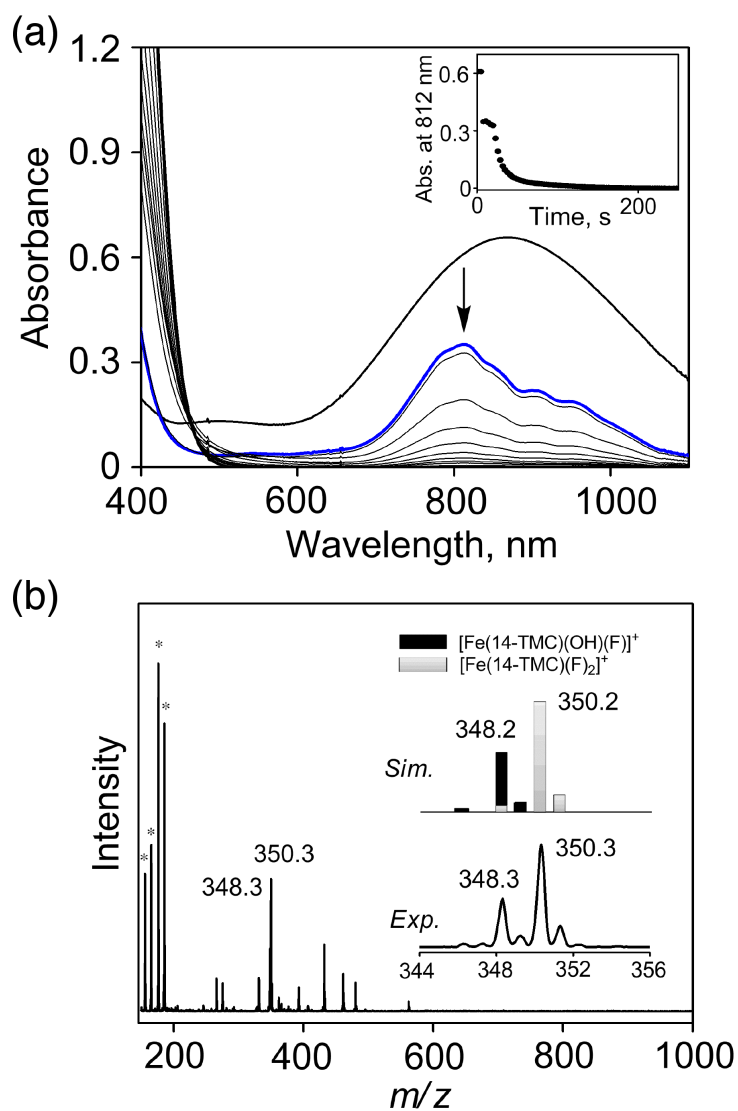


Fig. S2. (a) UV-vis spectral changes of the reaction of $[\text{Fe}^{\text{III}}(14\text{-TMC})(\text{O}_2)]^+$ (**1**) (1 mM) and 1.2 equiv. of NOPF_6 , followed by the addition of 2 equiv. of DTBP in CH_3CN at -10°C under Ar. Inset shows the time course of the absorbance at 812 nm. (b) ESI-MS spectrum of the resulting solution. Insets show the experimental (lower) and simulated (upper) spectra of the resulting solution in the region of m/z 344 – 356. The ion peaks at m/z of 348.3 and 350.3 correspond to $[\text{Fe}^{\text{III}}(14\text{-TMC})(\text{OH})(\text{F})]^+$ (**8**) and $[\text{Fe}^{\text{III}}(14\text{-TMC})(\text{F})_2]^+$, respectively. The peaks at m/z of 156.2, 165.6, 176.5, and 185.9 with an asterisk were assigned to $[\text{Fe}^{\text{II}}(14\text{-TMC})]^{2+}$, $[\text{Fe}^{\text{III}}(14\text{-TMC})(\text{F})]^{2+}$, $[\text{Fe}^{\text{II}}(14\text{-TMC})(\text{CH}_3\text{CN})]^{2+}$, and $[\text{Fe}^{\text{III}}(14\text{-TMC})(\text{CH}_3\text{CN})(\text{F})]^{2+}$, respectively.

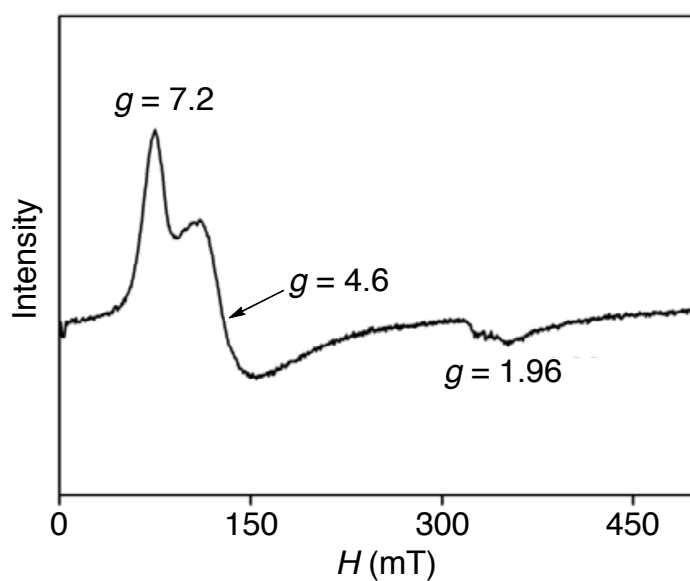


Fig. S3. EPR spectrum of the reaction solution of $[\text{Fe}^{\text{III}}(14\text{-TMC})(\text{O}_2)]^+$ (**1**) (1 mM) and 1.2 equiv. of NOPF_6 , followed by the addition of 2 equiv. of DTBP in frozen CH_3CN at 5 K. Experimental parameters: Power, 1.0 mW; Frequency, 9.647 GHz; Receive Gain, 1.0×10^4 ; Modulation Frequency, 100 kHz; Modulation Amplitude, 10 G.

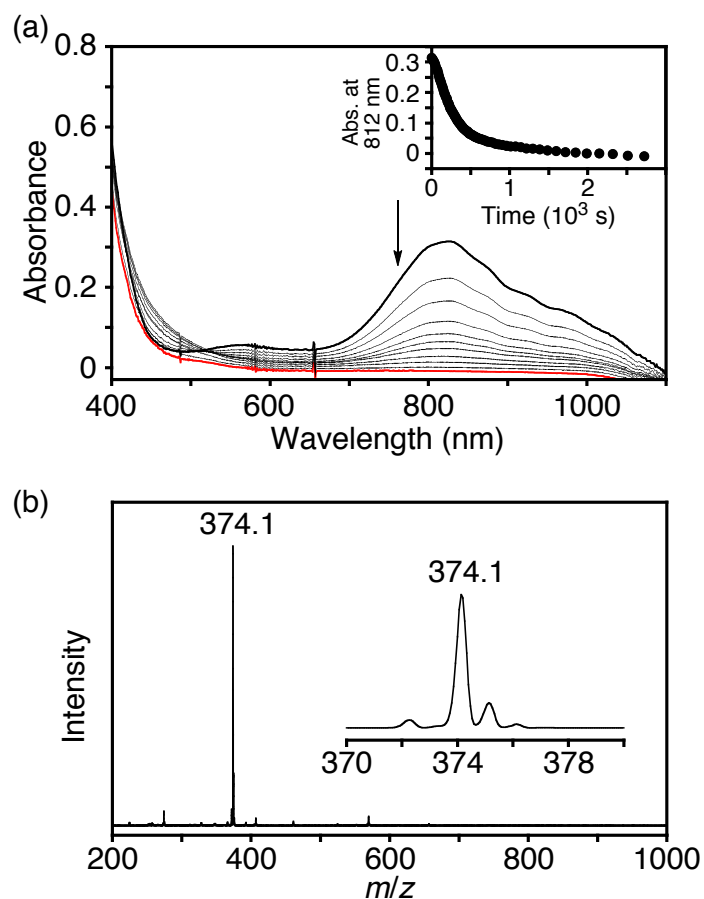


Fig. S4. (a) UV-vis spectral changes of $[\text{Fe}^{\text{IV}}(14\text{-TMC})(\text{O})(\text{CH}_3\text{CN})]^{2+}$ (1 mM) upon addition of NO_2 (5 equiv.) in CH_3CN at $-10\text{ }^\circ\text{C}$. (b) ESI-MS spectrum of the resulting solution. Inset shows the region of m/z 370 – 380. The ion peak at m/z of 374.1 corresponds to $[\text{Fe}^{\text{II}}(14\text{-TMC})(\text{NO}_3)]^+$ (calcd. m/z of 374.3).

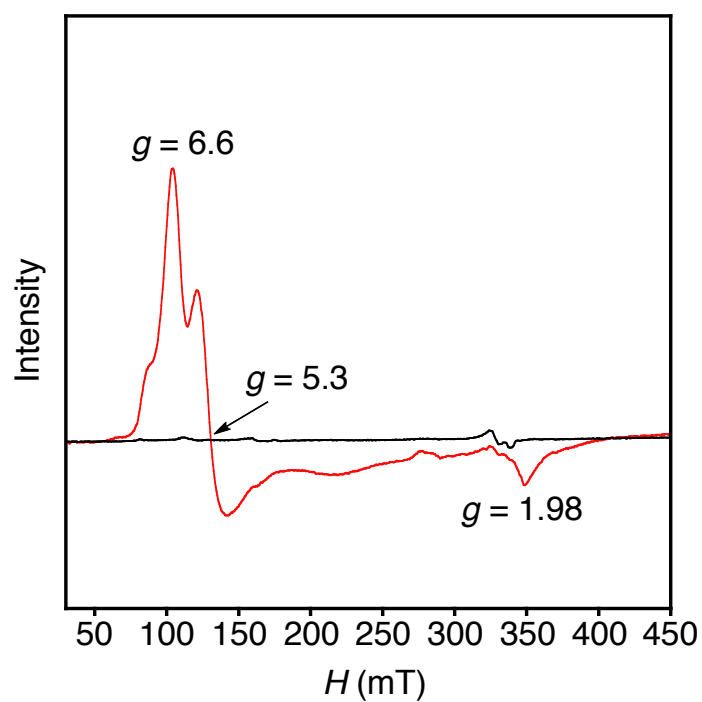


Fig. S5. EPR spectra of the reaction solution of $[\text{Fe}^{\text{IV}}(14\text{-TMC})(\text{O})(\text{CH}_3\text{CN})]^+$ (**5**) and 5 equiv. of NO_2 (black) and $[\text{Fe}^{\text{II}}(14\text{-TMC})(\text{NO}_3)]^+$ (**6**) with 1.2 equiv. of TBAF (red) in frozen CH_3CN at 5 K. Experimental parameters; Power, 1.0 mW; Frequency, 9.647 GHz; Receive Gain, 1.0×10^4 ; Modulation Frequency, 100 kHz; Modulation Amplitude, 10 G.

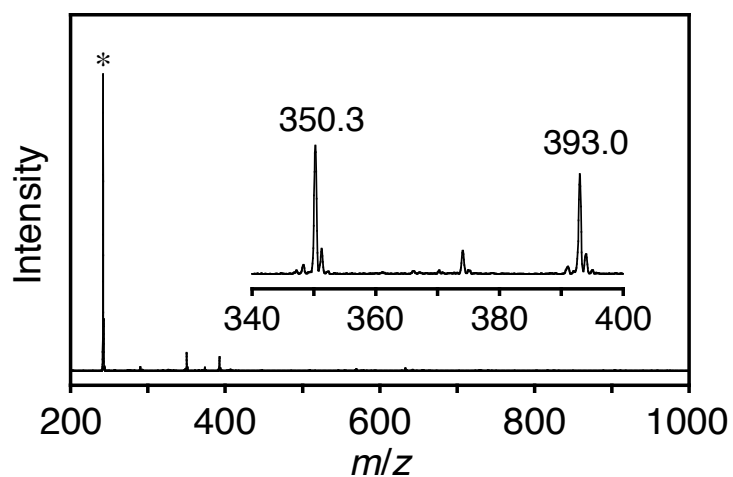


Fig. S6. ESI-MS spectrum of the reaction solution of $[\text{Fe}^{\text{II}}(14\text{-TMC})(\text{NO}_3)]^+$ (**5**) (1 mM) with TBAF (1.2 mM) in CH_3CN at $-10\text{ }^\circ\text{C}$. Inset shows the region of m/z 340 – 400. The ion peaks at m/z of 350.3 and 393.0 correspond to $[\text{Fe}^{\text{III}}(14\text{-TMC})(\text{F})_2]^+$ (calcd. m/z of 350.3) and $[\text{Fe}^{\text{III}}(14\text{-TMC})(\text{NO}_3)(\text{F})]^+$ (calcd. m/z of 393.3), respectively. The peak at m/z of 242.3 with asterisk was assigned to TBA^+ (tetrabutylammonium ion).

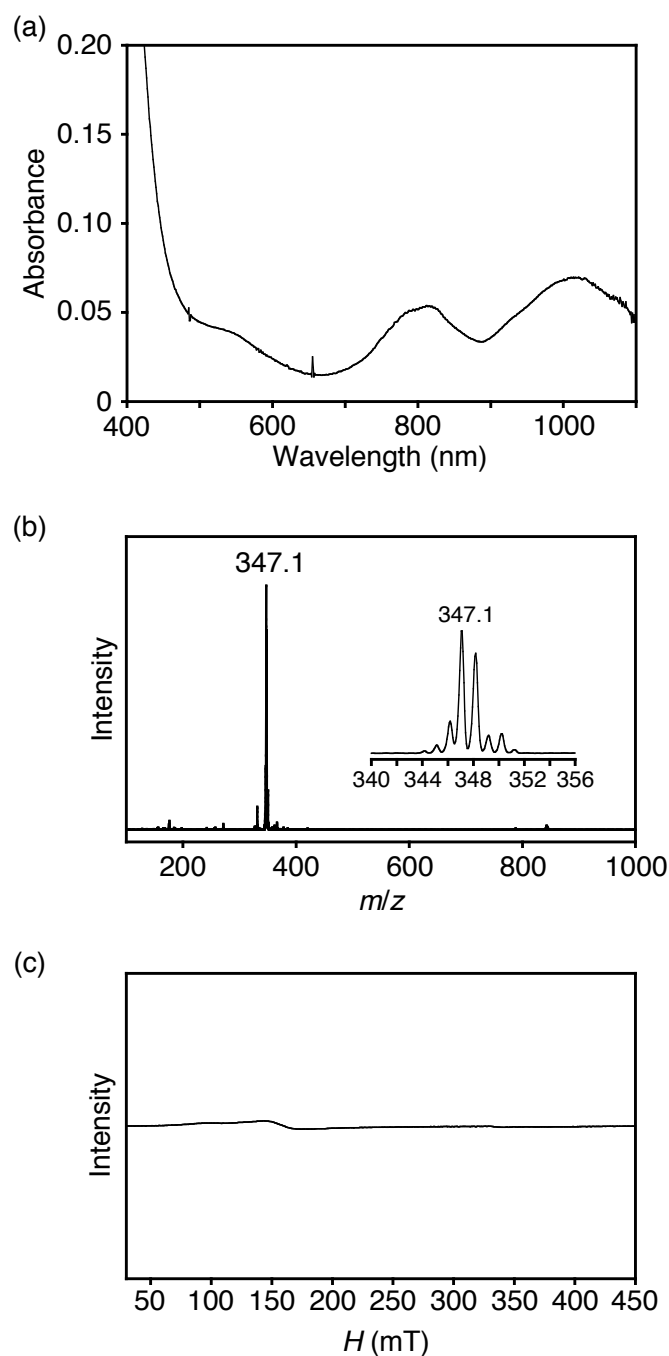


Fig. S7. (a) UV-vis spectrum of $[\text{Fe}^{\text{IV}}(14\text{-TMC})(\text{O})(\text{F})]^+$ (**7**) in CH_3CN (1 mM) at $-10\text{ }^\circ\text{C}$ under Ar. (b) ESI-MS spectrum of **7** (calcd. m/z of 347.2). Inset shows isotope distribution pattern for **7** at m/z of 347.1. (c) EPR spectrum of **7** in frozen CH_3CN at 5 K. Experimental parameters; Power, 1.0 mW; Frequency, 9.647 GHz; Receive Gain, 1.0×10^4 ; Modulation Frequency, 100 kHz; Modulation Amplitude, 10 G.

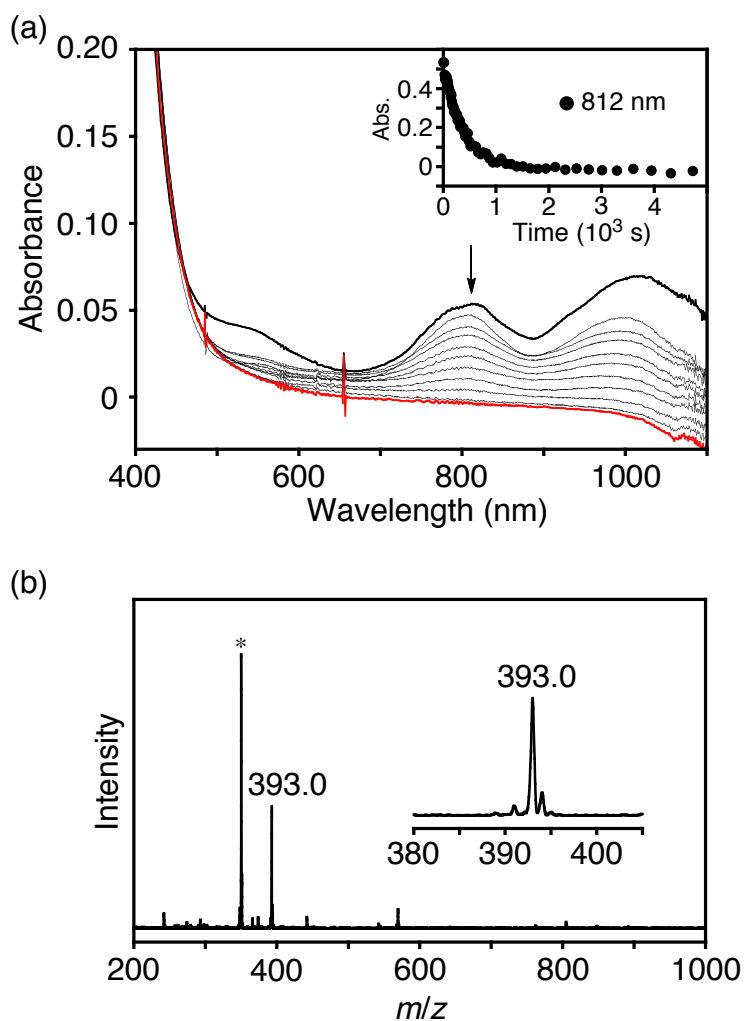


Fig. S8. (a) UV-vis spectral changes of $[\text{Fe}^{\text{IV}}(14\text{-TMC})(\text{O})(\text{F})]^+$ (**7**) (1 mM) upon addition of 5 equiv. of NO_2 in CH_3CN at -10°C under Ar. Inset shows time course of the absorbance change at 812 nm. (b) ESI-MS spectrum of the resulting solution. Inset shows the region of m/z 380 – 405. The ion peak at m/z of 393.0 corresponds to $[\text{Fe}^{\text{III}}(14\text{-TMC})(\text{NO}_3)(\text{F})]^+$ (calcd. m/z of 393.2). The peak at m/z of 350.2 with asterisk was assigned to $[\text{Fe}(14\text{-TMC})(\text{F})_2]^+$ (calcd. m/z of 350.2).

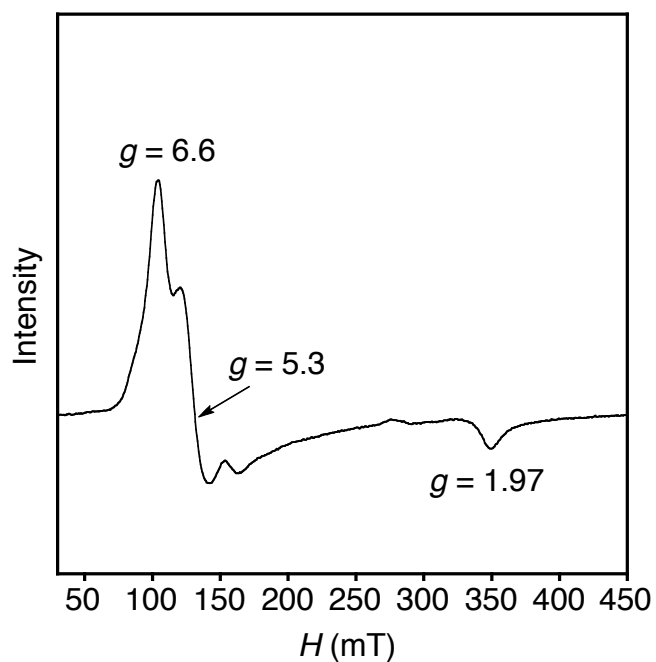


Fig. S9. EPR spectrum of the reaction solution of $[\text{Fe}^{\text{IV}}(14\text{-TMC})(\text{O})(\text{F})]^+$ (**7**) (1 mM) with 5 equiv. of NO_2 in frozen CH_3CN at 5 K. Experimental parameters; Power, 1.0 mW; Frequency, 9.647 GHz; Receive Gain, 1.0×10^4 ; Modulation Frequency, 100 kHz; Modulation Amplitude, 10 G.

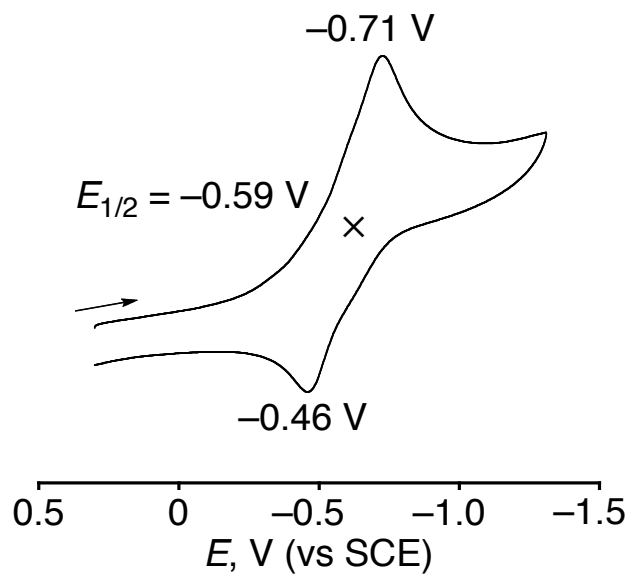


Figure S10. Cyclic voltammogram of $[\text{Fe}^{\text{IV}}(14\text{-TMC})(\text{O})(\text{F})](\text{OTf})$ (**7**) in CH_3CN at -10 °C under Ar in the presence of 0.1 M TBAPF_6 .